Dynamical symmetry breaking in a 2D electron gas with a spectral node

Klaus Ziegler[a]

Institut für Physik, Universität Augsburg, 86135 Augsburg, Germany

Abstract. We study a disordered 2D electron gas with a spectral node in a vicinity of the node. After identifying the fundamental dynamical symmetries of this system, the spontaneous breaking of the latter by a Grassmann field is studied within a nonlinear sigma model approach. This allows us to reduce the average two-particle Green's function to a diffusion propagator with a random diffusion coefficient. The latter has non-degenerate saddle points and is treated by the conventional self-consistent Born approximation. This leads to a renormalized chemical potential and a renormalized diffusion coefficient, where the DC conductivity increases linearly with the density of quasiparticles. Applied to the special case of Dirac fermions, our approach provides a comprehensive description of the minimal conductivity at the Dirac node as well as for the V-shape conductivity inside the bands.

1 Introduction

The prototype of a 2D electron gas with spectral nodes is graphene, where two symmetric electronic bands created by the underlying honeycomb lattice structure, touch each other at two different points in the Brillouin zone [1–4]. The surface states of the recently discovered topological insulators is another example for spectral nodes [5]. It is a remarkable experimental fact that the two-dimensional electron gas in graphene is always in a metallic state, regardless of its Fermi energy, provided that the sublattice symmetry of the honeycomb lattice is unbroken. This is particularly surprising from the theoretical point of view, since the electron gas should be in a localized state, at least away from the node (Dirac point) [6]. At the Dirac point, however, the underlying Hamiltonian has an extra particle-hole symmetry, depending on the type of disorder though, which may be responsible for metallic (diffusive) behavior. The experimentally observed metallic state at and away from the node indicates that the diffusive behavior may not depend on this extra symmetry. We shall discuss in the following that an additional dynamical symmetry exists which is responsible, regardless of the chemical potential, for a diffusive behavior.

Diffusion can only occur when random scattering is present in the system. This requires some kind of randomness in the Hamiltonian and the averaging of a physical quantity (e.g., the conductivity) with respect to the random distribution. A standard method for this procedure is the weak-localization approach (WLA) [7,8]. This method has been also applied to graphene [9–11] with the result that in the presence of only one Dirac node the system is metallic away from the node. This result has been later questioned, though, by Khveshchenko [12]. Unfortunately, the WLA of references [9–11] provides information only about whether or not weak disorder has the tendency to localize. Explicit expressions for the conductivity, which could be compared with experiments, are not available. Although the WLA and the method we shall describe in this paper are based on a weak-scattering expansion, there is a difference in how the long-range correlations are taken into account. The WLA uses the summation over maximally crossed diagrams [13], whereas we will extract massless modes from a spontaneously broken symmetry.

The paper is organized as follows: after introducing some fundamental quantities for the diffusion in a quantum system (Sect. 2), we discuss the symmetry properties of a two-band model in Section 3. Then we derive an effective nonlinear sigma model for the description of spontaneous symmetry breaking in our model (Sect. 3.1) and its treatment away from the node within perturbation theory (Sect. 3.2). This leads us to diffusion due to a massless mode, which is discussed and connected to transport properties of graphene in Section 4.

2 Quantum dynamics

Many characteristic properties of a quantum system, in particular the spectral and large scale properties, are determined by symmetry properties of the underlying Hamiltonian. However, for the dynamics of a quantum system additional symmetries play a role, because the dynamics is not only controlled by the real spectrum but also on the complex plane by the advanced and the retarded Green's function $G(\pm i\epsilon) = (H \pm i\epsilon)^{-1}$, which are related

[a] e-mail: ziegler@physik.uni-augsburg.de

by Hermitian conjugation: $G(-i\epsilon) = G^\dagger(i\epsilon)$. This plays a central role in the linear response approach to transport. But since linear response is quite complex in graphene [14], we will focus here on the transition probability [15]

$$P_{\mathbf{r},\mathbf{r}'}(i\epsilon) = K_{\mathbf{r},\mathbf{r}'}(i\epsilon) \Big/ \sum_{\mathbf{r}} K_{\mathbf{r},\mathbf{r}'}(i\epsilon) \tag{1}$$

with

$$K_{\mathbf{r},\mathbf{r}'}(i\epsilon) = \langle G_{\mathbf{r},\mathbf{r}'}(i\epsilon) G_{\mathbf{r}',\mathbf{r}}(-i\epsilon) \rangle_v \tag{2}$$

and return to the conductivity later. The average is here with respect to a random variable (e.g. random potential or a random gap) in the Hamiltonian H. Randomness is necessary to provide scattering that breaks translational invariance. It is convenient to combine the two Green's functions in the extended Green's function

$$\hat{G}(i\epsilon) = \begin{pmatrix} (H + i\epsilon)^{-1} & 0 \\ 0 & (H - i\epsilon)^{-1} \end{pmatrix} \tag{3}$$

such that with $\hat{H} = \mathrm{diag}(H, H)$ we have $\hat{G}(i\epsilon) = (\hat{H} + i\epsilon\hat{\sigma}_3)^{-1}$. Following the standard procedure for disordered systems, we must replicate this Hamiltonian, either using a fermion-boson pair or n fermion or boson replicas. Then there is an orthogonal or unitary symmetry which rotates the two-dimensional space that is spanned by the two Hamiltonians. It has been found long time ago that the symmetry breaking due to ϵ can cause spontaneous symmetry breaking in the limit $\epsilon \to 0$. The corresponding massless mode leads to a diffusive behavior [16,17].

The definition of (3) was also used as the starting point for Dirac fermions with random mass by Bocquet et al. [18]. Employing a supersymmetric representation, where $\hat{G}(i\epsilon)$ is applied to a Bose and to a Fermi field, the gradient expansion of the effective field theory produces an orthosymplectic nonlinear sigma model in this case. Unfortunately, the analysis of the latter is quite involved and the transport properties cannot be easily extracted.

Prior to the work by Bocquet et al., an alternative approach was suggested by the present author [19,20] using explicitly the fact that the Dirac Hamiltonian $H = i\sigma_k\partial_k + m\sigma_3$ (σ_j are Pauli matrices and ∂_j is the spatial (antisymmetric) difference operator with $\partial_j\varphi_{\mathbf{r}} = (\varphi_{\mathbf{r}+ae_j} - \varphi_{\mathbf{r}-ae_j})/a$, $a \sim 0$ is the lattice constant and e_j is the unit vector in j direction) obeys the relation

$$\sigma_1 H^T \sigma_1 = -H, \tag{4}$$

which constitutes class D according to references [21,22]. The relation enables us to introduce the structure

$$\hat{G}(i\epsilon) = \begin{pmatrix} (H + i\epsilon)^{-1} & 0 \\ 0 & (H^T - i\epsilon)^{-1} \end{pmatrix} \tag{5}$$

for the dynamic description. This choice has a very important advantage over (3), since the upper and the lower block have the same determinant. Then the upper block can act on bosons and the lower block on fermions, providing us with a Bose-Fermi field theory and a nonlinear sigma model that has only a free massless Fermi (Grassmann) field [19,20,23,24]. The latter describes diffusion and gives directly the experimentally observed minimal conductivity of graphene. Moreover, it reproduces the phase diagram (one metallic phase and two insulating Hall phases) of references [25–28] for a nonzero average mass [23,24].

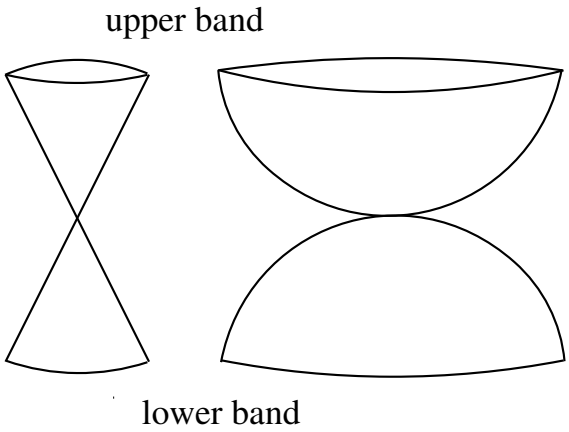

Fig. 1. Typical structure of two symmetric bands with a node with linear (left) and quadratic (right) dispersion.

The disadvantage of (5) over the definition (3) is its restriction to the Dirac point, since a shift by a chemical potential $H \to H + \mu\sigma_0$ violates the relation (4). To cure this limitation, we will start in the following from (5) and extend it in such a way that a chemical potential can be included [29]. This will give us a new dynamic structure with a continuous chiral symmetry in Bose-Fermi space. The latter can be spontaneously broken and produces a two-component massless Fermi (Grassmann) field.

We consider a Hamiltonian with two bands whose dispersion is symmetric: $\pm E(\mathbf{k})$ with the 2D wavevector $\mathbf{k}$. Moreover, we assume a generalized particle-hole symmetry for the Hamiltonian

$$UH^TU^\dagger = -H, \quad UU^\dagger = \mathbf{1}, \tag{6}$$

and include a node in the band structure (see Fig. 1). Besides the Dirac Hamiltonian of equation (4), where $H^T \neq H$ and $U = \sigma_1$, this includes also the symmetric chiral Hamiltonian $H = h_1\sigma_1 + h_2\sigma_2$, where $H^T = H$ and $U = \sigma_3$. An example is the tight-binding Hamiltonian on the honeycomb lattice. The latter consists of two triangular sublattices A and B, where nearest-neighbor hopping is always between sites on different sublattices. Thus, the hopping Hamiltonian reads

$$H = \begin{pmatrix} 0 & t_{BA} \\ t_{AB} & 0 \end{pmatrix} \tag{7}$$

with the hopping term t_{AB} (t_{BA}) from A to B (from B to A). Without a magnetic field the Hamiltonian is symmetric with $t_{BA} = t_{AB}^T$. This allows us to rewrite the Hamiltonian (7) in the form of $H = h_1\sigma_1 + h_2\sigma_2$ with $h_1 = (t_{AB} + t_{BA})/2$ and $h_2 = i(t_{AB} - t_{BA})/2$.

The existence of a node is important to create spontaneous symmetry breaking. This has been observed for gapped Dirac fermions, where the symmetry-breaking solution vanishes when the gap is too large [23,24].

3 General structure and symmetry

In analogy to the Green's function in equation (5) we introduce $\hat{G}(i\epsilon) = (\hat{H}+i\epsilon)^{-1}$ with the extended Hamiltonian

$$\hat{H} = \begin{pmatrix} H_+ & 0 & 0 & 0 \\ 0 & H_- & 0 & 0 \\ 0 & 0 & H_-^T & 0 \\ 0 & 0 & 0 & H_+^T \end{pmatrix}, \quad H_\pm = H \pm \mu\sigma_0. \tag{8}$$

Then, together with property (6), the matrix

$$\hat{S} = \begin{pmatrix} 0 & 0 & \varphi_1 U & 0 \\ 0 & 0 & 0 & \varphi_2 U \\ \varphi_1' U^\dagger & 0 & 0 & 0 \\ 0 & \varphi_2' U^\dagger & 0 & 0 \end{pmatrix} \tag{9}$$

with scalar variables φ_j, φ_j' anticommutes with $\hat{H}$: $\hat{S}\hat{H} = -\hat{H}\hat{S}$. This relation implies a non-Abelian chiral symmetry [19,20,29]:

$$e^{\hat{S}}\hat{H}e^{\hat{S}} = \hat{H} \tag{10}$$

which is a symmetry relation for the extended Hamiltonian with respect to $\hat{U} = e^{\hat{S}}$.

Interpretation of the non-Abelian chiral transformation: The anticommuting property $\hat{S}\hat{H} = -\hat{H}\hat{S}$ implies the appearance of two conjugate energy bands with energies $\pm E$, respectively, where the eigenstate $|-E\rangle$ is created from the eigenstate $|E\rangle$ through the relation $\hat{S}|E\rangle \propto |-E\rangle$ due to

$$\hat{H}\hat{S}|E\rangle = -\hat{S}\hat{H}|E\rangle = -E\hat{S}|E\rangle.$$

Iteration of this relation provides the relation $\hat{S}^n|E\rangle \propto |(-1)^n E\rangle$. Thus, $e^{\hat{S}}|E\rangle$ is a linear superposition of states in the upper and lower band $|\pm E\rangle$ with the property

$$\langle E'|e^{\hat{S}}\hat{H}e^{\hat{S}}|E\rangle = \langle E'|\hat{H}|E\rangle = E\delta_{E',E},$$

i.e., the Hamiltonian matrix is diagonal with respect to the states $e^{\hat{S}}|E\rangle$, where the diagonal elements are the energies. In other words, the variables φ, φ' in $\hat{S}$ create a two-dimensional manifold of states for which the Hamiltonian matrix is invariant. Moreover, we can define eigenstates to the operator $\hat{S}$ as: $|\pm S\rangle = |E\rangle \pm |-E\rangle$, which have the eigenvalues ± 1. These eigenvalues characterize the chirality of these states.

Furthermore, for the eigenstate $|E\rangle$ of $\hat{H}$ the state $e^{\hat{S}}|E\rangle$ is eigenstate of $\hat{H}^2$ with eigenvalue E^2 due to:

$$\begin{aligned}\hat{H}^2 e^{\hat{S}}|E\rangle &= e^{\hat{S}}e^{-\hat{S}}\hat{H}e^{-\hat{S}}e^{\hat{S}}\hat{H}e^{\hat{S}}|E\rangle = e^{\hat{S}}\hat{H}^2|E\rangle \\ &= E^2 e^{\hat{S}}|E\rangle. \end{aligned} \tag{11}$$

These results indicate that the variables φ, φ' describe an adiabatic change from $|E\rangle$ to $|-E\rangle$. The corresponding manifold is non-compact, as we can see in the following example of two Dirac fermions with random gap (cf. Sect. 2) and complex φ and its complex conjugate φ'. In this case the matrices read

$$\hat{S} = \begin{pmatrix} 0 & \varphi\sigma_1 \\ \varphi'\sigma_1 & 0 \end{pmatrix}, \quad e^{\hat{S}} = \begin{pmatrix} c\sigma_0 & e^{i\phi}s\sigma_1 \\ e^{-i\phi}s\sigma_1 & c\sigma_0 \end{pmatrix},$$

$$c = \cosh|\varphi|, \quad s = \sinh|\varphi|, \quad \phi = \arg(\varphi) \tag{12}$$

where the variables c, s parametrize a non-compact manifold. This is reminiscent of the hyperbolic saddle-point manifold discovered in the bosonic replica approach to disordered electronic systems, which is the foundation of the nonlinear sigma model description for Anderson localization [16].

Now we use the matrix structure of (8) and apply it to a superspace that consists of four bosonic (upper) components and four fermionic (lower) components. In this representation $\varphi_{1,2}$, $\varphi_{1,2}'$ in (9) are Grassmann variables, and we have to introduce the graded determinant detg and the graded trace Trg (cf. [23,24]). The reason for using a superspace is that for constructing the functional integral of the transition matrix K in equation (2) it is crucial to have the properties $\mathrm{detg}(\hat{H}+i\epsilon) = 1$ and $\mathrm{detg}(e^{\hat{S}}) = \exp(\mathrm{Trg}\hat{S}) = 1$ [29]. Therefore, the symmetry is a supersymmetry, connecting bosonic with fermionic degrees of freedom. This symmetry is broken by the ϵ term, though, because $\hat{U}^2$ is not a unit matrix. Equations (8)–(10) are the main results of this work. What remains to be discussed is the effect of the symmetry property on the transport for $\epsilon \to 0$, which will be studied by the standard nonlinear sigma model approach [16,17,30].

3.1 Nonlinear sigma model

The symmetry (10) is valid for any random H or μ, provided that H obeys (6). In order to calculate K of equation (2) it is necessary to specify the details of the randomness. Once this has been done, it is convenient to employ a transformation from the random variables of the Hamiltonian (e.g., random gap or random chemical potential) to the distribution of the diagonal elements of the Green's function $G_{\mathbf{r},\mathbf{r}}(\pm i\epsilon)$. The resulting functional integral can be treated within a saddle-point approximation.

Without repeating here the lengthy and technical but straightforward derivation of the functional integral (cf. [23,24]), we switch directly to the saddle-point approximation of the integral, which allows us to focus on the role of the symmetry in equation (10). For this purpose, we start from a special saddle-point solution (which is equivalent to the self-consistent Born approximation of the average one-particle Green's function [12])

$$\langle(\hat{H}+i\epsilon)^{-1}\rangle \approx (\langle\hat{H}\rangle + i\epsilon + i\eta)^{-1} \equiv \hat{G}_0, \tag{13}$$

where the scattering rate η is determined for disorder with strength g by the self-consistent equation $\eta = 2ig\hat{G}_{0,0}$ [19,20,31], and perform the functional integration only with respect to the symmetry transformation (9), independently at each site $\mathbf{r}$. This requires that we replace the two parameters φ_j $(j = 1, 2)$ by the space-dependent Grassmann fields $\varphi_{j\mathbf{r}}$ such that the integration reduces to the invariant measure, defined through the Jacobian

$$J = \mathrm{detg}\left(\langle \hat{H}\rangle + i\epsilon + i\eta\hat{U}^2\right)^{-1}. \tag{14}$$

Thus K of equation (2) reads:

$$K_{\mathbf{r}\mathbf{r}'} \approx 4\frac{\eta^2}{g^2}\sum_{j=1,2}\int \varphi_{j\mathbf{r}}\varphi'_{j\mathbf{r}'}J\mathcal{D}[\varphi,\varphi'], \tag{15}$$

where we have summed over j, since the diffusion is the same for $\pm\mu$.

Next we expand $-\log J$ in powers of the scattering rate η. This is also an expansion in powers of $\hat{G}_0$, as defined in equation (13), which is convergent on large scales [29]. Up to second order in η it reads $-\log J = S'' + o(\eta^3)$ with

$$S'' = i\eta\mathrm{Trg}\left(\hat{G}_0\hat{U}^2\right) - \frac{\eta^2}{2}\mathrm{Trg}\left[\left(\hat{G}_0\hat{U}^2\right)^2\right].$$

This is the nonlinear sigma model for the nonlinear field $\hat{U}^2 = e^{2\hat{S}}$. Using the definition of the latter field in Section 3, this can also be expressed by the field $\hat{S}$ as:

$$\begin{aligned} S'' = {} & 4i\eta\mathrm{Trg}\left(\hat{G}_0\hat{S}^2\right) - 8\eta^2\mathrm{Trg}\left[\left(\hat{G}_0\hat{S}\right)^2\right] \\ & - 8\eta^2\mathrm{Trg}\left[\left(\hat{G}_0\hat{S}^2\right)^2\right], \end{aligned} \tag{16}$$

where the off-diagonal parts of the last two terms give the standard form of the nonlinear sigma model [30], and the first term and the diagonal part of the second term contribute to the symmetry-breaking term that is proportional to ϵ. Evaluating the three expansion terms (cf. Appendix A) leads to S'' which separates into two components as $S'' = S''_1 + S''_2$ with

$$S''_j = \frac{4\eta}{g}\sum_{\mathbf{r}}\left[\varphi_{j\mathbf{r}}(\epsilon - D\partial^2)\varphi'_{j\mathbf{r}} + \alpha_j\Phi_{j\mathbf{r}}\partial^2\Phi_{j\mathbf{r}}\right], \tag{17}$$

with the composite field $\Phi_{j\mathbf{r}} = \varphi_{j\mathbf{r}}\varphi'_{j\mathbf{r}}$ and with the Laplacian $\partial^2 = \partial_1^2 + \partial_2^2$. With the Green's function $g_\pm = [\langle H\rangle + i(\epsilon + \eta) \pm \bar{\mu}]^{-1}$ the parameters read for $\epsilon \sim 0$

$$\alpha = -\frac{\eta^2}{2}\mathrm{Tr}_2\left(\mathrm{g}^2_{+,0} - \mathrm{g}^2_{-,0}\right) = -\mathrm{i}\eta^2\mathrm{ImTr}_2(\mathrm{g}^2_{+,0}), \tag{18}$$

$\alpha_j = -(-1)^j\alpha$ and an isotropic diffusion coefficient

$$D = -\frac{g\eta}{2}\frac{\partial^2}{\partial q_1^2}\int_{\mathbf{k}}\mathrm{Tr}_2[\tilde{\mathrm{g}}_{+,\mathbf{k}}(\mathrm{i}\eta)\tilde{\mathrm{g}}_{+,\mathbf{k}-\mathbf{q}}(-\mathrm{i}\eta)]\Big|_{q=0}, \tag{19}$$

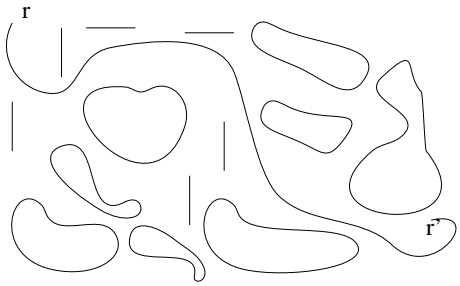

Fig. 2. A schematic representation of the expansion in equation (21). The random walk of an electron connecting the sites $\mathbf{r}$ and $\mathbf{r}'$ and the loops come from the adjugate, whereas the dimers originate from the expansion terms around the node.

where $\tilde{g}_{\pm,\mathbf{k}}$ are the Fourier components of the Green's function $g_\pm$ and Tr_2 is the trace with respect to Pauli matrices. Thus our model depends only on the parameters g (disorder strength), η (scattering rate), and the renormalized chemical potential $\bar{\mu}$. Interestingly, α vanishes for $\bar{\mu} = 0$ such that the interaction disappears at the node (cf. [19,20]). This enables us to employ an expansion of $J \approx \exp(-S'')$ in powers of α to study the behavior of the integral (15) away from the node.

According to (8) and (9), different values of j refer to different Fermi energies: $(H + i\epsilon + \mu)^{-1}$ (for $j = 1$) and $(H + i\epsilon - \mu)^{-1}$ (for $j = 2$). The different signs in front of α in equation (17) reflect the fact that α is proportional to μ. In the following we ignore the index j because its value affects only the sign of the coupling constant.

3.2 Perturbation theory around the node

At $\alpha = 0$ the unperturbed integral simply reads as the adjugate of $\epsilon - D\partial^2$:

$$K_{\mathbf{r},\mathbf{r}'} = \det(\epsilon - D\partial^2)(\epsilon - D\partial^2)^{-1}_{\mathbf{r},\mathbf{r}'} \equiv Adj_{\mathbf{r},\mathbf{r}'}(\epsilon - D\partial^2). \tag{20}$$

The perturbation expansion on the real space Λ then becomes (cf. Appendix C)

$$K_{\mathbf{r},\mathbf{r}'} = \sum_I Adj^I_{\mathbf{r},\mathbf{r}'}(\epsilon - D\partial^2)\prod'_{\mathbf{r}'',\mathbf{r}'''\in\Lambda\setminus I}\alpha_j\partial^2_{\mathbf{r}'',\mathbf{r}'''}, \tag{21}$$

where $Adj^I_{\mathbf{r},\mathbf{r}'}(\epsilon - D\partial^2)$ is the adjugate on the subspace $I \subseteq \Lambda$, the perturbation is on its complement $\Lambda\setminus I$, and the summation is over all subspaces I.

The expansion in equation (21) can also be understood as a random-walk expansion, where the perturbation $\alpha_j\Phi_{j\mathbf{r}}\partial^2\Phi_{j\mathbf{r}}$ represent a "dimer" on the lattice which cannot be visited by the random walk (diffusive path) because of the Grassmann variables. In other words, the perturbation blocks dimers on the lattice which are not accessible for the random walk, and the actual walk takes place only on the sites that are not blocked by dimers (cf. Appendix C and Fig. 2). This restricts the random walk of the electron but since the walk has no phase factor (it is a classical random walk since $\epsilon - D\partial^2$ is a real

symmetric matrix, as explained in Appendix C), there is no interference to generate Anderson localization.

Here it should be noticed that a hopping expansion of the two-particle Green's function (2) would also give a random-walk expansion but with random phase terms. This reflects the quantum character of our system. In particular, the random phase fluctuations can lead to cancellations of expansion terms which may eventually cause Anderson localization. Unfortunately, such an expansion is difficult to control. The approach of this article, in which we have extracted the behavior on large scales in the form of a nonlinear sigma model, allows us to connect the system away from the node with the system at the node $\mu = 0$ by a classical random walk. Since no interference appears in classical random walks, our extraction of the massless modes simplifies the calculation substantially.

In reference [32] we have applied a renormalization-group procedure directly to the action (17) and found that the interaction term scales to zero on large scales. In the following we employ the perturbation expansion of equation (21) as an alternative approach which will lead us to a similar result. It is based on the idea that the interaction can be treated within the self-consistent Born approximation [9–11,31] by replacing the diffusion coefficient at the node D as $D \to \bar{D}_j = D + (-1)^j D'$. This can be understood as a partial summation of our expansion in equation (21), where $(-1)^j D'$ is a self-energy. This approximation should be reliable, since there is no continuous degeneracy of the self-consistent solutions, in contrast to the supersymmetric functional integral of equation (15). In the special case of the Dirac Hamiltonian $\langle H \rangle = i\sigma_k \partial_k$ (valid for a single node in graphene or for the surface of a topological insulator) we get from equation (19), after performing the $\mathbf{k}$ integral, the expression [33]

$$D = \frac{g}{8\pi\eta}\left[1 + \frac{1+\zeta^2}{\zeta}\arctan\zeta\right], \quad \zeta = \bar{\mu}/\eta. \tag{22}$$

For given g and μ the renormalized parameters η and $\bar{\mu}$ are determined as a solution of a self-consistent approach (cf. Appendix B) with

$$D' \sim \alpha\lambda^2/4\pi D, \quad \alpha \sim -i\frac{\bar{\mu}}{\eta(1+\eta^2/\lambda^2)},$$

where λ is the momentum cut-off. The Fourier components of $P_{\mathbf{r}} \equiv P_{\mathbf{r}0}$ in equation (1) then read

$$\tilde{P}_{\mathbf{q}} = \tilde{K}_{\mathbf{q}}/\tilde{K}_0 = \frac{\epsilon(\epsilon + Dq^2)}{(\epsilon + Dq^2)^2 + D'^2 q^4} \tag{23}$$

and the diffusive expansion of the wavefunction $\sum_{\mathbf{r}} r_k^2 P_{\mathbf{r}}$ is

$$-\tilde{K}''_{\mathbf{q}=0}/\tilde{K}_{\mathbf{q}=0} = 2D/\epsilon. \tag{24}$$

It should be noticed that the correction D' drops out and only the diffusion coefficient D enters the final result. As a result, D is plotted in Figure 3.

Although the dynamic conductivity is quite complex for Dirac particles [14], the DC conductivity can be extracted from the Einstein relation as

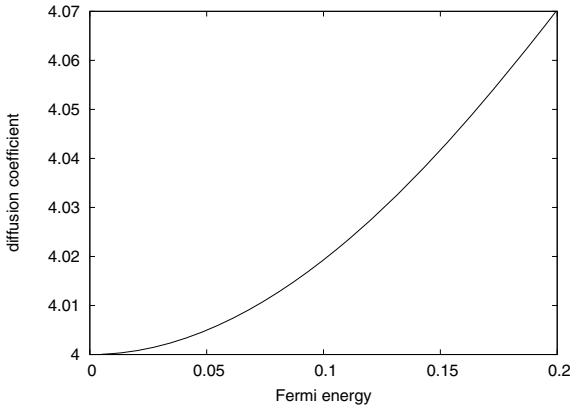

Fig. 3. Diffusion coefficient for 2D Dirac fermions (in arbitray units) as a function of the renormalized chemical potential $\bar{\mu}$ for $g = 1$ (from Eq. (22)).

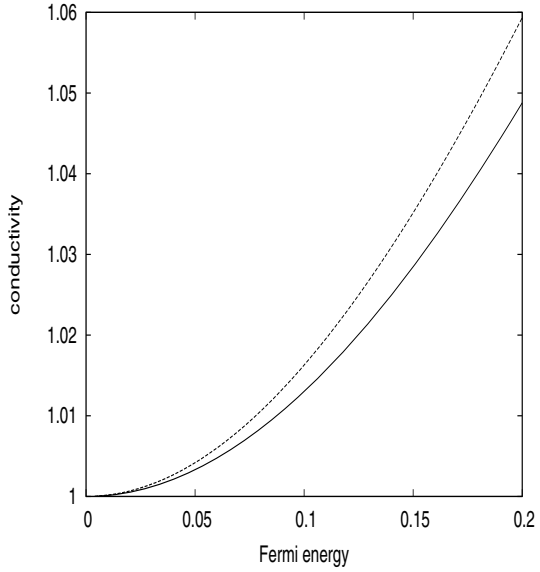

Fig. 4. The conductivity in units of $e^2/\pi h$ as a function of the Fermi energy μ (from Eq. (26)) for $g = 0.8$ (dashed curve) and for $g = 1$ (full curve).

$$\sigma_{kk} \propto \rho D\frac{e^2}{h} \tag{25}$$

with the density of states at the Fermi level ρ. In fact, the Kubo conductivity [23,24] gives

$$\sigma_{kk}(\mu, 0) = 4\frac{e^2}{h}\frac{\eta}{g}D = \frac{e^2}{2\pi h}\left[1 + \frac{1+\zeta^2}{\zeta}\arctan\zeta\right], \tag{26}$$

where ζ is a function of the Fermi energy μ and can be calculated self-consistently (cf. Appendix B). The result is plotted in Figure 4. The conductivity increases with $|\bar{\mu}|^2$. This, on the other hand, is proportional to the quasiparticle density n. Consequently, the conductivity increases linearly with n. This behavior is in agreement with the experimental observation of a V-shaped

Table 1. Comparison of the WLA [9–11] and the CSBA for physical quantities of a single Dirac node. g is measured in units of the squared Fermi velocity v^2 and we have used $\zeta = \bar{\mu}\tau/\hbar$. The function $t(\mu)$ can be taken from equation (B.2) and must be calculated from the self-consistent equation (B.1). It starts from 1 for $\mu = 0$, is roughly $1/\mu^2$ in a crossover region and roughly $1/\mu$ for $\mu \gg 0$.

	WLA	CSBA
Diffusion coefficient D	$v^2\tau$	$\frac{g\tau}{8\pi}\left[1+\frac{1+\zeta^2}{\zeta}\arctan\zeta\right]$
Conductivity σ	$\frac{8e^2}{hg\tau}D+\frac{4e^2}{\pi h}\log(l_\phi/2v\tau)$	$\frac{4e^2}{hg\tau}D$
Scattering time τ	$2\hbar v^2/g\mu$	$t(\mu)e^{v^2/g}$

conductivity [1,2,34,35]. In the pure limit without scattering ($\eta \to 0$) we get from equation (22) for the diffusion coefficient $D \to \infty$ and from equation (26) for the conductivity

$$\sigma_{kk} \to \begin{cases} e^2/\pi h & \text{for } \mu = 0 \\ \infty & \text{for } \mu \neq 0. \end{cases}$$

Thus, at the Dirac node the quantum fluctuations are sufficient to create a finite conductivity, while away from the node scattering is necessary to obtain a finite conductivity.

4 Discussion

The calculation of transport properties near the Dirac node (e.g. in graphene) has been discussed at length in the literature, using the weak-localization approximation (WLA) [9–11]. In order to understand the connection to our result, in particular in terms of the conductivity in equation (26), we briefly survey the Kubo approach within our symmetry-breaking picture and compare it with the WLA.

Starting from the Kubo formula [7,8,23,24]

$$\sigma_{kk} = -\frac{e^2}{2h}\omega^2 \lim_{\epsilon\to 0} \times \mathrm{Re}\left\{\sum_{\mathbf{r}} \mathrm{r_k^2 Tr_2}\left[\langle \mathrm{G_{0\mathbf{r}}}(\omega/2+\mathrm{i}\epsilon)\mathrm{G_{\mathbf{r}0}}(-\omega/2-\mathrm{i}\epsilon)\rangle\right]\right\}, \tag{27}$$

we could employ an approximation for the average two-particle Green's function by factorizing the averaged product as [7,8]

$$\langle G_{0\mathbf{r}}(y)G_{\mathbf{r}0}(-y)\rangle \approx \langle G_{0\mathbf{r}}(y)\rangle\langle G_{\mathbf{r}0}(-y)\rangle \quad (y = \omega/2 + i\epsilon), \tag{28}$$

which neglects the correlations between the two Green's functions at $\pm y$. This can be combined with the self-consistent Born approximation in equation (13) to obtain

$$\langle G_{0\mathbf{r}}(y)\rangle\langle G_{\mathbf{r}0}(-y)\rangle \approx G_{0,\mathbf{r}}(y+i\eta)G_{0,-\mathbf{r}}(-y-i\eta). \tag{29}$$

This gives the leading term of the WLA, namely the Boltzmann (or Drude) conductivity [7–11]. However, this approximation ignores the long-range correlations of the average two-particle Green's function that is required for diffusion, since $G_{0,\mathbf{r}}(y+i\eta)$ decays exponentially on the scale $1/\eta$. Consequently, the sum on the right-hand side of equation (27) is finite. Now the main result of the chiral symmetry-breaking approach (CSBA) is that it extracts the long-range behavior of the average two-particle Green's function in form of the massless mode, described approximately by the nonlinear sigma model (17). This implies that the approximations in equations (28), (29) are replaced by the relation [23,24]

$$\sum_{\mathbf{r}} r_k^2 \mathrm{Tr}_2\left[\langle G_{0\mathbf{r}}(y)G_{\mathbf{r}0}(-y)\rangle\right] = (1+i\eta/y)^2 \times \sum_{\mathbf{r}} r_k^2 \mathrm{Tr}_2\left[G_{0,\mathbf{r}}(y+i\eta)G_{0,-\mathbf{r}}(-y-i\eta)\right], \tag{30}$$

where the coefficient on the right-hand side represents correlations of the fluctuating Green's functions on large scales. These correlations are negligible only for $\omega\tau \gg 1$ ($\tau = \hbar/\eta$ is the scattering time). Inserting relation (30) into the conductivity, we obtain a correction term proportional to η^2 in comparison with the factorization approximation. An alternative way to evaluate these corrections for the conductivity consists of the summation of certain diagrams from the perturbation theory. An example is maximally crossed diagrams [13], which is the foundation of the WLA. In Table 1 we compare several physical quantities for a single Dirac node (i.e., for the long-range potential in the notion of Refs. [9–11]), either calculated in weak-localization approximation (WLA) or in our CSBA. The WLA requires a phenomenological cut-off on the length scale l_ϕ that is justified by inelastic scattering. Such a cut-off does not appear in the CSBA due to the absence of logarithmic singularities.

The results of both approaches agree well on a qualitative level for $\mu \gg 0$: $D \propto \tau$, $\sigma \approx$ const. and $\tau \propto \mu^{-1}$. On the other hand, for small Fermi energies close to the Dirac point, where the WLA is not reliable [9–11], there is a significant deviation. In this regime the CSBA approach should also be reliable, as long as disorder is not too strong. It gives $D \approx g\tau/4\pi$, $\sigma \approx e^2/\pi h$ and $\tau \approx e^{v^2/g}$ (v is the Fermi velocity). The disagreement between the results of the two approaches near the Dirac node can be explained by the fact that the WLA is based on choosing a special subclass of diagrams of the perturbation theory. For 2D Dirac fermions, however, we have seen that

there is a cancellation of the logarithmically divergent diagrams in each order if all diagrams are considered [36]. In contrast to the WLA, the CSBA projects onto the chiral symmetry-breaking modes first and then uses an expansion in powers of $\eta = \hbar/\tau$ in the exponent of the Jacobian. This may explain the different results for the two approaches in Table 1.

Both approaches involve certain approximations which cannot be justified directly because they are based on the truncation of a perturbation series. For instance, the CSBA neglects the massive (short-range correlated) fluctuations of the Green's functions, and the WLA takes into account only the maximally crossed diagrams. Thus, although both approaches are systematic, they lead to different results. They can be understood as new well-defined models for transport, describing different physical situations. This brings us in the position to compare their respective results with experimental observations. Transport properties of disordered two-dimensional Dirac fermions have been studied intensively in the case of graphene. The conductivity is characterized by its robust minimal value at the Dirac node $\mu = 0$ with $\sigma_{min} \approx 4e^2/h$ (the factor 4 is the result of a four-fold degeneracy due to the spin and two valleys). Away from the Dirac node the conductivity increases with μ^2 [1] and with a prefactor that decreases with the disorder strength [34]. On the other hand, the theoretical results in Table 1 give an infinite negative minimal conductivity for the WLA and $\sigma_{min} = 4e^2/\pi h$ (taking into account the four-fold degeneracy) for the CSBA. Besides the factor $1/\pi$, the CSBA agrees quite well with the experiments. It should be noticed though that the WLA is not reliable near the Dirac node, as mentioned above. Away from the Dirac node the WLA gives a conductivity that increases logarithmically with the Fermi energy μ, in contrast to the parabolic increase of the CSBA result in Figure 4. Moreover, the WLA correction of the conductivity increases logarithmically with disorder strength g, whereas the CSBA conductivity decreases with increasing g (cf. Fig. 4). These results indicate clearly that the CSBA agrees much better with the experimental observations.

5 Conclusions

We have found that the transport properties of a 2D electron gas with a spectral node are controlled by a non-Abelian chiral symmetry. Spontaneous breaking of the symmetry generates massless fermion modes that lead to diffusion: one mode if the system is at the node and two modes if the system is away from the node. We have argued that the system away from the node is connected with the system at the node $\mu = 0$ by a classical random walk. The latter can be approximated by a self-consistent approach. This reproduces the result that there is no renormalization of the bare diffusion coefficient, which was recently found in a renormalization-group calculation of this problem [32].

The knowledge of the diffusion coefficient enabled us to calculate the DC conductivity via the Einstein relation. We have also seen that this is a good approximation for the Kubo formula. For the special case of two-dimensional Dirac fermions this calculation reproduces the well-known V shape of the density-conductivity plot in graphene. Therefore, our work explains the experimentally observed linear DC conductivity away from the charge neutrality point (Dirac node), and provides a description that is an alternative to the effect of charged disorder [37].

Finally, it should be mentioned that the approximation in equation (16) corresponds to a weak scattering expansion in powers of the scattering rate η. If we apply a strong scattering expansion in powers of $1/\eta$ we would see Anderson localization [38]. In this regime strong fluctuations due to disorder destroy the massless modes and create an exponentially decaying correlation function on the scale $\hbar v_F/\eta$. However, this requires a scattering rate of the order of the band width, which is too large to be realized for most physical systems.

In summary, we have described the transport in a two-dimensional two-band system, using spontaneous breaking of a non-Abelian chiral symmetry. As an extension of previous calculations, our approach is applicable not only at the (Dirac) node but also inside the two bands. With this we found a systematic description which applies also to transport in graphene. In particular, we were able within a single approach to obtain (i) the minimal conductivity at the Dirac nodes and (ii) the V-shape conductivity inside the bands that is linear in the density of charge carriers.

I am grateful to A. Sinner for interesting discussions. This work was supported through the DFG grant ZI 305/5-1.

Appendix A: Coefficients of the nonlinear sigma model

The expansion terms in equation (16) read

$$\mathrm{Trg}\left(\hat{G}_0\hat{S}^2\right) = \mathrm{tr}\left[(\mathrm{g}_+ + \mathrm{g}_-)(\varphi_1\varphi_1' + \varphi_2\varphi_2')\right], \qquad \text{(A.1)}$$

where tr is the trace with respect to the sites and the Pauli matrices.

$$\mathrm{Trg}\Big[\left(\hat{G}_0\hat{S}\right)^2\Big] = \mathrm{Trg}\Big[\hat{G}_0\hat{S}\hat{G}_0\hat{S}\Big] = 2\Big[\mathrm{tr}(\mathrm{g}_+\varphi_1\mathrm{U}\mathrm{g}_-^{\mathrm{T}}\varphi_1'\mathrm{U}^\dagger) + \mathrm{tr}(g_-\varphi_2 U g_+^T\varphi_2' U^\dagger)\Big] \qquad \text{(A.2)}$$

and

$$\mathrm{Trg}\Big[\left(\hat{G}_0\hat{S}^2\right)^2\Big] = \mathrm{Trg}\Big[\hat{G}_0\hat{S}^2\hat{G}_0\hat{S}^2\Big] = -\sum_{j=1,2}(-1)^j\Big[\mathrm{tr}(\mathrm{g}_+\varphi_\mathrm{j}\varphi_\mathrm{j}'\mathrm{g}_+\varphi_\mathrm{j}\varphi_\mathrm{j}') - \mathrm{tr}(\mathrm{g}_-\varphi_\mathrm{j}\varphi_\mathrm{j}'\mathrm{g}_-\varphi_\mathrm{j}\varphi_\mathrm{j}')\Big] \qquad \text{(A.3)}$$

Moreover, for $\bar{\eta} = \eta + \epsilon$ we have

$$U g_\pm(i\bar{\eta})^T U^\dagger = -g_\mp(-i\bar{\eta}) \qquad \text{(A.4)}$$

such that we get from equation (A.2)

$$\mathrm{Trg}\left[\hat{G}_0\hat{S}\hat{G}_0\hat{S}\right] = -2\mathrm{tr}\left[\mathrm{g}_+(\mathrm{i}\bar{\eta})\varphi_1\mathrm{g}_+(-\mathrm{i}\bar{\eta})\varphi_1'\right] - 2\mathrm{tr}\left[\mathrm{g}_-(\mathrm{i}\bar{\eta})\varphi_2\mathrm{g}_-(-\mathrm{i}\bar{\eta})\varphi_2'\right]. \quad \text{(A.5)}$$

Now we assume that the Grassmann field $\varphi_{j,\mathbf{r}}$ varies only on large scales. This allows us to expand the expressions (A.1)–(A.3) in powers of the wave vector $\mathbf{q}$ up to second order. Then we have, together with the property $UU^\dagger = \mathbf{1}$,

$$\mathrm{tr}\left[\mathrm{g}_\pm(\mathrm{i}\bar{\eta})\right] = -\mathrm{tr}\left[\mathrm{g}_\mp(-\mathrm{i}\bar{\eta})\right],$$
$$\mathrm{tr}\left[\mathrm{g}_+(\mathrm{i}\bar{\eta}) + \mathrm{g}_-(\mathrm{i}\bar{\eta})\right] = \mathrm{tr}\left[\mathrm{g}_+(\mathrm{i}\bar{\eta}) - \mathrm{g}_+(-\mathrm{i}\bar{\eta})\right]$$

and

$$\mathrm{tr}\left[\mathrm{g}_\pm(\mathrm{i}\bar{\eta}) - \mathrm{g}_\pm(-\mathrm{i}\bar{\eta})\right] = -2\mathrm{i}\bar{\eta}\mathrm{tr}\left[\mathrm{g}_\pm(\mathrm{i}\bar{\eta})\mathrm{g}_\pm(-\mathrm{i}\bar{\eta})\right]$$

such that

$$\mathrm{tr}\left[\mathrm{g}_+(\mathrm{i}\bar{\eta}) + \mathrm{g}_-(\mathrm{i}\bar{\eta})\right] = -2\mathrm{i}\bar{\eta}\mathrm{tr}\left[\mathrm{g}_\pm(\mathrm{i}\bar{\eta})\mathrm{g}_\pm(-\mathrm{i}\bar{\eta})\right].$$

This gives us equation (17) with the coefficients (18), (19).

Appendix B: Self-consistent calculation of the scattering rate

The scattering rate $\eta = 1/\tau$ is a function of the Fermi energy μ and can be evaluated within the self-consistent equation $\eta = 2igG_{0,0}(z + i\eta)$ which reads for small g

$$\frac{g\nu}{\mu} = \frac{e^{-\kappa\tan\kappa}\cos\kappa}{\kappa} \quad (-\pi/2 < \kappa < \pi/2) \quad \nu = \lambda e^{-1/g}. \quad \text{(B.1)}$$

This equation determines κ and the latter gives

$$\eta = \nu e^{\kappa\tan\kappa}\cos\kappa, \quad \frac{\bar{\mu}}{\eta} = \frac{g\kappa + \cos\kappa\sin\kappa}{\cos^2\kappa}. \quad \text{(B.2)}$$

Appendix C: Random walk expansion

The random walk expansion is a convenient tool to calculate the integral of equation (15) [39]. In our case it leads to a perturbation series in powers of α_j. It is be based on the expansion of $\exp(-S_j'')$ with S_j'' given in equation (17):

$$\exp(-S_j'') = \exp\left(\sum_{\mathbf{r}}\varphi_{j\mathbf{r}}(\epsilon - D\partial^2)\varphi_{j\mathbf{r}}'\right) \times \prod_{\mathbf{r}}\left(1 + \alpha_j\varphi_{j\mathbf{r}}\varphi_{j\mathbf{r}}'\partial^2\varphi_{j\mathbf{r}}\varphi_{j\mathbf{r}}'\right). \quad \text{(C.1)}$$

For this result and for the following discussion it is crucial to keep in mind that Grasmann variables are nilpotent (i.e., $\varphi_{j\mathbf{r}}^n = \varphi_{j\mathbf{r}}'^n = 0$ for integer $n > 1$). From the definition $\partial_j\Phi_{\mathbf{r}} = (\Phi_{\mathbf{r}+ae_j} - \Phi_{\mathbf{r}-ae_j})/a$ we get $\partial_j^2\Phi_{\mathbf{r}} = (\Phi_{\mathbf{r}+2ae_j} + \Phi_{\mathbf{r}-2ae_j} - 2\Phi_{\mathbf{r}})/a^2$. First we notice that

$$\varphi_{j\mathbf{r}}\varphi_{j\mathbf{r}}'\partial^2\varphi_{j\mathbf{r}}\varphi_{j\mathbf{r}}' = -\varphi_{j\mathbf{r}}\varphi_{j\mathbf{r}}'\frac{1}{a^2} \times \sum_{n=1,2}(\varphi_{j\mathbf{r}+2ae_n}\varphi_{j\mathbf{r}+2ae_n}' + \varphi_{j\mathbf{r}-2ae_n}\varphi_{j\mathbf{r}-2ae_n}').$$

Thus, the second factor in (C.1) provides at each pair of sites (dimer) $\mathbf{r}, \mathbf{r} \pm 2ae_n$ either a factor 1 or a product of Grassmann variables $\varphi_{j\mathbf{r}}\varphi_{j\mathbf{r}}'\varphi_{j\mathbf{r}\pm2ae_n}\varphi_{j\mathbf{r}\pm2ae_n}'$, respectively. This allows us to write

$$\exp(-S_j'') = \exp\left(\sum_{\mathbf{r}\in\Lambda}\varphi_{j\mathbf{r}}(\epsilon - D\partial^2)\varphi_{j\mathbf{r}}'\right) \times \sum_I \prod_{\mathbf{r},\mathbf{r}'\in I}{}' \frac{\alpha_j}{a^2}\varphi_{j\mathbf{r}}\varphi_{j\mathbf{r}}'\varphi_{j\mathbf{r}'}\varphi_{j\mathbf{r}'}', \quad \text{(C.2)}$$

where the product $\prod'_{\mathbf{r},\mathbf{r}'\in I}$ is restricted to dimers $\mathbf{r}' = \mathbf{r} \pm 2ae_n$ and $I \subseteq \Lambda$ is a subset of our real space Λ. Next we can expand the first factor in (C.1) by using

$$\sum_{\mathbf{r}\in\Lambda}\varphi_{j\mathbf{r}}(\epsilon - D\partial^2)\varphi_{j\mathbf{r}}' = (\epsilon + 2D_a)\sum_{\mathbf{r}\in\Lambda}\varphi_{j\mathbf{r}}\varphi_{j\mathbf{r}}' - D_a$$
$$[1.5mm]\times\sum_{\mathbf{r}\in\Lambda}\sum_{n=1,2}\varphi_{j\mathbf{r}}(\varphi_{j\mathbf{r}+2ae_n}' + \varphi_{j\mathbf{r}-2ae_n}') \quad (D_a = D/a^2)$$

such that

$$\exp\left(\sum_{\mathbf{r}\in\Lambda}\varphi_{j\mathbf{r}}(\epsilon - D\partial^2)\varphi_{j\mathbf{r}}'\right) = \exp\left((\epsilon + 2D_a)\sum_{\mathbf{r}\in\Lambda}\varphi_{j\mathbf{r}}\varphi_{j\mathbf{r}}'\right) \times \sum_{I'}\prod_{\mathbf{r},\mathbf{r}'\in I'}{}'\left(-D_a\varphi_{j\mathbf{r}}\varphi_{j\mathbf{r}'}'\right).$$

Combining the expansion of the two factors in equation (C.1) gives us

$$\exp(-S_j'') = \sum_{I,I'}\prod_{\mathbf{r}\in\Lambda}[1 + (\epsilon + 2D_a)\varphi_{j\mathbf{r}}\varphi_{j\mathbf{r}}']\prod_{\mathbf{r},\mathbf{r}'\in I}{}' \times \left(-D_a\varphi_{j\mathbf{r}}\varphi_{j\mathbf{r}'}'\right)\prod_{\mathbf{r},\mathbf{r}'\in I'}{}'\frac{\alpha_j}{a^2}\varphi_{j\mathbf{r}}\varphi_{j\mathbf{r}}'\varphi_{j\mathbf{r}'}\varphi_{j\mathbf{r}'}'. \quad \text{(C.3)}$$

I and I' must be disjunct (i.e., they have no common sites $\mathbf{r}$) to give a non-zero contribution to the sum due to the nilpotent Grassmann variables. Thus, the approximated Jacobian $\exp(-S_j'')$ consists of (I) factors $\frac{\alpha_j}{a^2}\varphi_{j\mathbf{r}}\varphi_{j\mathbf{r}}'\varphi_{j\mathbf{r}'}\varphi_{j\mathbf{r}'}'$ from dimers $\mathbf{r}, \mathbf{r}' \in I'$, (II) factors $-D_a\varphi_{j\mathbf{r}}\varphi_{j\mathbf{r}'}'$ from dimers $\mathbf{r}, \mathbf{r}' \in I$ and (III) factors $(\epsilon + 2D_a)\varphi_{j\mathbf{r}}\varphi_{j\mathbf{r}}'$ on points $\mathbf{r}$, which do neither belong to I' nor to I. Inserting this result into the correlation function of equation (15), we can perform the integration over the Grassmann variables for each term of the sums in equation (C.3). At each site $\mathbf{r}$ the integral gives 1 if there is a factor $\varphi_{j\mathbf{r}}\varphi_{j\mathbf{r}}'$ and zero otherwise. Then the result of the

expansion can be represented in a graphical manner: since there are only isolated points (with $(\epsilon + 2D_a)$), isolated dimers (with α_j/a^2) or connected dimers (with $-D_a$) after the Grassmann integration, we can depict these three types of elements as isolated points, isolated dimers and connected dimers in space, respectively. We also have to take into account the extra Grassmann variables in the integrand $\varphi_{j\mathbf{r}}\varphi'_{j\mathbf{r}'}$. They can only appear as end points of a chain of connected dimers, as it is shown in Figure 2. The other connected dimers form closed loops and cannot intersect with each other.

Equation (C.3) is identical to

$$\begin{aligned}\exp(-S''_j) &= \sum_I \prod_{\mathbf{r}\in I}[1+(\epsilon+2D_a)\varphi_{j\mathbf{r}}\varphi'_{j\mathbf{r}}]\prod'_{\mathbf{r},\mathbf{r}'\in I}\\ &\quad\times\left(1-D_a\varphi_{j\mathbf{r}}\varphi'_{j\mathbf{r}'}\right)\prod'_{\mathbf{r},\mathbf{r}'\in\Lambda\setminus I}\frac{\alpha_j}{a^2}\varphi_{j\mathbf{r}}\varphi'_{j\mathbf{r}}\varphi_{j\mathbf{r}'}\varphi'_{j\mathbf{r}'}\\ &= \sum_I \exp\left(\sum_{\mathbf{r}\in I}\varphi_{j\mathbf{r}}(\epsilon - D\partial^2)\varphi'_{j\mathbf{r}}\right)\\ &\quad\times\prod'_{\mathbf{r},\mathbf{r}'\in\Lambda\setminus I}\frac{\alpha_j}{a^2}\varphi_{j\mathbf{r}}\varphi'_{j\mathbf{r}}\varphi_{j\mathbf{r}'}\varphi'_{j\mathbf{r}'}. \qquad \text{(C.4)}\end{aligned}$$

Inserting this into equation (15) and performing the integration with respect to the Grassmann variables gives us equation (21).

References

1. K.S. Novoselov, A.K. Geim, S.V. Morozov, D. Jiang, M.I. Katsnelson, I.V. Grigorieva, S.V. Dubonos, A.A. Firsov, Nature **438**, 197 (2005)
2. Y. Zhang, Y.-W. Tan, H.L. Stormer, P. Kim, Nature **438**, 201 (2005)
3. A.H. Castro Neto, F. Guinea, N.M.R. Peres, K.S. Novoselov, A.K. Geim, Rev. Mod. Phys. **81**, 109 (2009)
4. D.S.L. Abergel, V. Apalkov, J. Berashevich, K. Ziegler, T. Chakraborty, Adv. Phys. **59**, 261 (2010)
5. X.-L. Qi, S.-C. Zhang, Rev. Mod. Phys. **83**, 1057 (2011)
6. E. Abrahams, P.W. Anderson, D.C. Licciardello, T.V. Ramakrishnan, Phys. Rev. Lett. **42**, 673 (1979)
7. B.L. Altshuler et al., Phys. Rev. B **22**, 5142 (1980)
8. B.L. Altshuler, B.D. Simons, in *Mesoscopic quantum physics*, edited by E. Akkermans et al. (North-Holland, Amsterdam, 1995)
9. T. Ando, Y. Zheng, H. Suzuura, J. Phys. Soc. Jpn **71**, 1318 (2002)
10. H. Suzuura, T. Ando, Phys. Rev. Lett. **89**, 266603 (2002)
11. E. McCann et al., Phys. Rev. Lett. **97**, 146805 (2006)
12. D.V. Khveshchenko, Phys. Rev. Lett., **97**, 036802 (2006)
13. J.S. Langer, T. Neal, Phys. Rev. Lett. **16**, 984 (1966)
14. M. Lewkowicz, B. Rosenstein, Phys. Rev. Lett. **102**, 106802 (2009)
15. E.N. Economou, M.H. Cohen, Phys. Rev. Lett. **25**, 1445 (1970)
16. L. Schäfer, F. Wegner, Z. Physik B **38**, 113 (1980)
17. K. Efetov, *Supersymmetry in Disorder and Chaos* (Cambridge University Press, Cambridge, 1997)
18. M. Bocquet, D. Serban, M.R. Zirnbauer, Nucl. Phys. B **578**, 628 (2000)
19. K. Ziegler, Phys. Rev. B **55**, 10661 (1997)
20. K. Ziegler, Phys. Rev. Lett. **80**, 3113 (1998)
21. M.R. Zirnbauer, J. Math. Phys. **37**, 4986 (1996)
22. A. Altland, M.R. Zirnbauer, Phys. Rev. B **55**, 1142 (1997)
23. K. Ziegler, Phys. Rev. Lett. **102**, 126802 (2009)
24. K. Ziegler, Phys. Rev. B **79**, 195424 (2009)
25. T. Senthil, M.P.A. Fisher, Phys. Rev. B **61**, 9690 (2000)
26. J.T. Chalker, N. Read, V. Kagalovsky, B. Horovitz, Y. Avishai, A.W.W. Ludwig, Phys. Rev. B **65** 012506 (2001)
27. F. Evers, A.D. Mirlin, Rev. Mod. Phys. **80**, 1355 (2008)
28. M.V. Medvedyeva, J. Tworzydlo, C.W.J. Beenakker, Phys. Rev. B **81**, 214203 (2010)
29. K. Ziegler, J. Phys. A **45**, 335001 (2012)
30. S. Coleman, *Aspects of Symmetry* (Cambridge University Press, Cambridge, 1985)
31. N.H. Shon, T. Ando, J. Phys. Soc. Jpn **67**, 2421 (1998)
32. A. Sinner, K. Ziegler, Phys. Rev. B **86**, 155450 (2012)
33. J.Z. Bernád, U. Zülicke, K. Ziegler, Physica E **42**, 755 (2010)
34. J.H. Chen, C. Jang, M.S. Fuhrer, E.D. Williams, M. Ishigami, Nat. Phys. **4**, 377 (2008)
35. E.Y. Andrei, G. Li, X. Du, Rep. Prog. Phys., **75**, 056501 (2012)
36. A. Sinner, K. Ziegler, Phys. Rev. B **84**, 233401 (2011)
37. K. Nomura, A.H. MacDonald, Phys. Rev. Lett. **96**, 256602 (2006)
38. A. Hill, K. Ziegler, `arXiv:1305.6901` (2013)
39. J. Glimm, A. Jaffe, *Quantum Physics* (Springer-Verlag, New York, 1981)